Biomed Microdevices (2013) 15:997–1003
DOI 10.1007/s10544-013-9791-7

Superparamagnetic microrobots: fabrication by two-photon polymerization and biocompatibility

Marcel Suter · Li Zhang · Erdem C. Siringil · Christian Peters · Tessa Luehmann · Olgac Ergeneman · Kathrin E. Peyer · Bradley J. Nelson · Christofer Hierold

Published online: 12 July 2013

Abstract This work presents the fabrication and controlled actuation of swimming microrobots made of a magnetic polymer composite (MPC) consisting of 11-nm-diameter magnetite (Fe_3O_4) nanoparticles and photocurable resin (SU-8). Two-photon polymerization (TPP) is used to fabricate the magnetic microstructures. The material properties and the cytotoxicity of the MPC with different nanoparticle concentrations are characterized. The live/dead staining tests indicate that MPC samples with varied concentrations, up to 10 vol.%, have negligible cytotoxicity after 24 h incubation. Fabrication parameters of MPC with up to 4 vol.% were investigated. We demonstrate that the helical microdevices made of 2 vol.% MPC were capable of performing corkscrew motion in water applying weak uniform rotating magnetic fields.

Keywords Superparamagnetic nanocomposite · Microrobots · Magnetic actuation · Cytotoxicity

Electronic supplementary material The online version of this article (doi:10.1007/s10544-013-9791-7) contains supplementary material, which is available to authorized users.

M. Suter · C. Peters · C. Hierold
Micro and Nano Systems, ETH Zurich, Zurich, Switzerland

L. Zhang (✉)
Department of Mechanical and Automation Engineering,
The Chinese University of Hong Kong,
Shatin NT, Hong Kong SAR, China
e-mail: lizhang@mae.cuhk.edu.hk

E. C. Siringil · O. Ergeneman · K. E. Peyer · B. J. Nelson
Institute of Robotics and Intelligent Systems,
ETH Zurich, Zurich, Switzerland

T. Luehmann
Institute for Pharmacy and Food Chemistry,
University of Wurzburg, Wurzburg, Germany

1 Introduction

Recent advances in biomedicine and biology attract researchers to use remotely controlled micro-/nanodevices and systems that enable wireless manipulation and sensing for *in vivo* and *in vitro* applications (Ozin et al. 2005; Shi et al. 2009; Fan et al. 2010; Sing et al. 2010; Hagiwara et al. 2011; Mei et al. 2011; Ghosh and Fischer 2009; Solovev et al. 2012; Wang 2012; Peyer et al. 2013a). In particular, microrobotics in combination with different disciplines such as material science and micro-/nanofabrication technologies has opened new routes for minimally invasive medicine (Nelson et al. 2010; Qiu et al. 2012). For remote actuation of micro-/nanodevices with on-demand locomotion, magnetic actuation is a promising approach, because it works in various media, and is considered safe for cells and biological systems. The movement of miniaturized objects in liquid environments experience a relative increase in drag forces, since the Reynolds number significantly decreases due to the small characteristic length of the object (Purcell 1977). Swimming strategies at small scales can be adapted from the motion of bacteria such as *Escherichia coli* (*E. coli*). They rotate a bundle of helical-shaped flagella by 40-nm-diameter flagellar rotary motors to achieve a forward swimming movement (Anderson and Berg 1973). For a magnetic helical swimming microrobot, a more straightforward method to generate the corkscrew motion is to induce a magnetic torque on the device using a rotating magnetic field. However, the fabrication of such helical micro-/nanostructures is a challenge, and biocompatibility has to be considered for biomedical applications. Various designs of helical swimming microrobots have been reported, including artificial bacterial flagella (ABF) containing a hybrid semiconductor–metal trilayer (GaAs/InGaAs/Cr) with soft-magnetic Ni heads (Zhang et al. 2009a), helical micromachines coated with Ni/Ti thin films using e-beam evaporation (Tottori et al. 2012; Peyer et al. 2013b), and

helical lipid microstructures coated with CoNiReP thin films by electroless deposition (Schuerle et al. 2012). For fabrication and magnetic actuation of swimming microrobots, magnetic nanoparticles, such as superparamagnetic iron oxide nanoparticles (SPION), can be considered. They have a high degree of biocompatibility and provide possibilities for functionalization and tracking when used as *in vivo* targeted drug delivery systems (Lu et al. 2007; Kim et al. 2008; Colombo et al. 2012). Previous report also shows that flagellated magnetotactic bacteria (MTB) with the nanometer-sized magnetosomes can be used as magnetic microrobots in the human microvasculature (Martel et al. 2009).

In this work, two-photon photopolymerization (TPP) (Park et al. 2009; Tian et al. 2010; Zhang et al. 2010a) for three-dimensional (3-D) patterning of magnetic polymer composite (MPC) structures, composed of SU-8 photoresist and 11-nm-diameter magnetite (Fe_3O_4) nanoparticles, are presented. The material properties and the cytotoxicity of the MPC with different particle concentrations are also investigated. In addition, the magnetic actuation and swimming of the fabricated magnetic helical microrobots using low-strength rotating magnetic fields is demonstrated. While the fabrication and magnetic actuation of tethered MPC microdevices on a surface was reported (Tian et al. 2010; Xia et al. 2010), this work focuses on the fabrication of untethered devices for biomedical applications with an emphasis on the influence of the particle concentration on the feature size of 3D structures and cytotoxicity.

2 Results and discussion

2.1 Characterization of the composite

The magnetic composite is made of epoxy SU-8 polymer containing magnetite nanoparticles with diameters of 11.4±3.4 nm (average diameter measured by TEM) (Suter et al. 2011a). The particle agglomeration in the composite is one of the most significant issues for the fabrication of microstructures to obtain homogeneous magnetic and mechanical properties and small feature sizes. Figure 1 shows a cross-section of the composite film with 2 vol.% nanoparticle concentration. It was found that the nanoparticle agglomeration in the composite has an average size of around 40–50 nm and the composite shows superparamagnetic behavior (Suter et al. 2011a).

The biocompatibility of the MPC is important to evaluate the potential of MPC microdevices interfacing cells and biological systems. The cytotoxicity of the MPC with different particle concentrations was studied by WST-1 proliferation assay. A live and dead staining of normal human dermalfibroblasts (NHDFs) cultured on MPC surfaces was performed as previously described (Sivaraman et al. 2012).

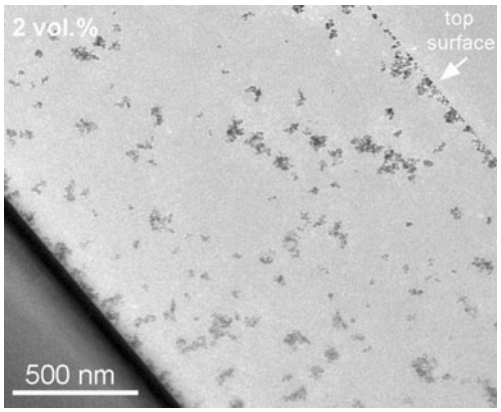

Fig. 1 TEM image of a cross-section of a spin-coated MPC film with 2 vol.% (8 wt.%) Fe_3O_4 particle concentration (sample thickness ≈ 100 nm)

The live and dead staining experiment shows that after a culture period of 24 h, NHDFs attached on all MPC samples and were able to metabolize FDA (Fig. 2a) independent of the Fe_3O_4 nanoparticle concentration. For a qualitative cytotoxicity analysis the mitochondrial activity of the living cells was measured on different MPC surfaces after 24 h (Fig. 2b). The cell viability for all samples was nearly the same as on control TCPS surfaces, indicating that nanoparticle concentrations up to 10 vol.% in the composite do not significantly influence the viability of NHDFs. MPC microstructures with up to 10 vol.% nanoparticle concentration are suitable for *in vitro* interactions with biomaterials.

2.2 Microstructure fabrication using two-photon polymerization

The fabrication of MPC microstructures using TPP allows for 3-D shape designs and the thickness of the polymerized photoresist is increased due to the longer wavelength as compared to standard UV photolithography. With UV photolithography at 350–410 nm the MPC has a low transmittance and the fabrication is limited to layer thickness of 2.9 μm for a composite with 5 vol.% (i.e. approximate 15 wt.%) magnetite concentration (Suter et al. 2011b). At a wavelength of 780 nm, i.e. the wavelength of the TPP laser, the transparence of MPC is significantly increased (see Electronic Supplementary Information—ESI, Figure S1). For instance, the transmittance of the MPC with 5 vol.% particle concentration is increased by approximately one order of magnitude as the wavelength of exposure is increased from i-line (365 nm) to 780 nm TPP laser and the maximum achievable thickness of the structures is increased by almost one order of magnitude. These observations are comparable to those made during the investigation of single photon visible light curing systems for SU-8 based polymer composites (Peters et al. 2013).

With TPP it is possible to precisely write structures smaller than the wavelength limitations (Zhang et al. 2010a). Here,

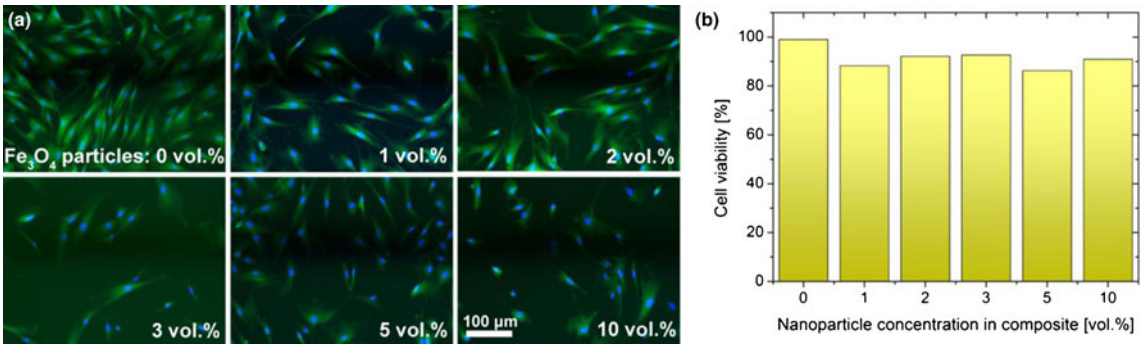

Fig. 2 **a** Epi-fluorescence microscope images of NDHFs cultured on MPC surfaces containing different Fe_3O_4 nanoparticle concentrations. *Green* fluorescence is from live cells while *blue* fluorescence is from cell nuclei. **b** With a WST-1 assay the viability of NDHFs was determined by the mitochondrial activity of living cells compared to a control tissue culture polystyrene (TCPS). The cell viability is normalized to values of cells cultured on TCPS. The *graph* represents average values from two independent experiments carried out in duplicates (except for 3 vol.% MPC only one measurement)

magnetic lines with widths down to 295±25 nm and 268±37 nm were fabricated using superparamagnetic composite (Fig. 3) for 2, and 4 vol.% nanoparticle concentrations, respectively. To achieve minimal feature size the scanning speed and laser power parameters were adjusted.

Constant scanning speed, as shown in Table 1, with decreasing laser power leads to thinner MPC lines until the composite cannot be fully polymerized and the lines are removed during the development process. For different laser-scanning-speed/laser-power combinations minimal feature sizes were investigated. For a 2 vol.% MPC the average of the obtained minimal line widths is 325±24 nm and for the line height 1.36±0.22 µm (see ESI, Table S1). For the 4 vol.% MPC only minimal line widths for different scanning-speed/laser-power combinations were investigated and was found as 287±16 nm. The minimal line widths depend only slightly on the nanoparticle concentrations. The decrease of the line width with higher particle concentrations can be due to the increased laser light absorption of the nanoparticles.

TPP allows for the fabrication of complex magnetic 3-D bulk microstructures by writing with parallel slightly overlapping lines (Peters et al. 2013). Figure 4a,b shows a hollow cube with dimensions of 20×20×20 µm, with a 2 µm thick wall and four 10×10 µm windows. Such hollow structures show the potential of this technology for example to fabricate open magnetic capsules for drug transportation (Frances et al. 2008). Objects up to 25 µm tall were fabricated using MPC with 2 vol.% particle concentration. Figure 4c and e show successfully fabricated helical microstructures with 2 and 4 vol.% Fe_3O_4 nanoparticle concentration. Helical microstructures with the MPC with heights up to 16.8 µm can be written by the laser following helical trajectories. The height and width of the filament can be defined by the number of neighboring trajectories. A line overlap of around 50 % in the vertical and horizontal directions was chosen. Because of the overlap the writing power can be slightly reduced compared to the minimal line writing parameters. The optimized parameters for the fabricated helical microstructures are 0.8 mW, 5 µm/s and 0.8 mW, 1 µm/s for 2 and 4 vol.% Fe_3O_4 nanoparticle concentrations, respectively. If the particle concentration is increased, the surface roughness of the helical microstructures increases due to the radiation absorption and scattering by the nanoparticles and their agglomerates.

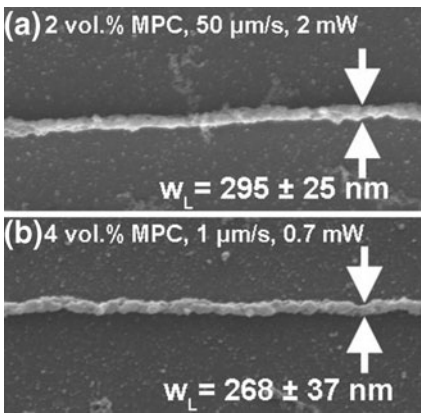

Fig. 3 MPC lines with minimal line width fabricated with (**a**) 2 vol.% and (**b**) 4 vol.% Fe_3O_4 nanoparticle concentration

2.3 Magnetic actuation of helical swimming microrobots

The fabricated MPC helical microstructures show corkscrew swimming capabilities in water when a magnetic torque is applied by a uniform rotating magnetic field. The

Table 1 Line width for different laser power values using 2 vol.% MPC (values from 3 to 10 measurements)

Scanning-speed/laser-power	Minimal line width
50 µm/s, 2.4 mW	382±56 nm
50 µm/s, 2.2 mW	321±58 nm
50 µm/s, 2.0 mW	295±25 nm
50 µm/s, 1.8 mW	no stable line

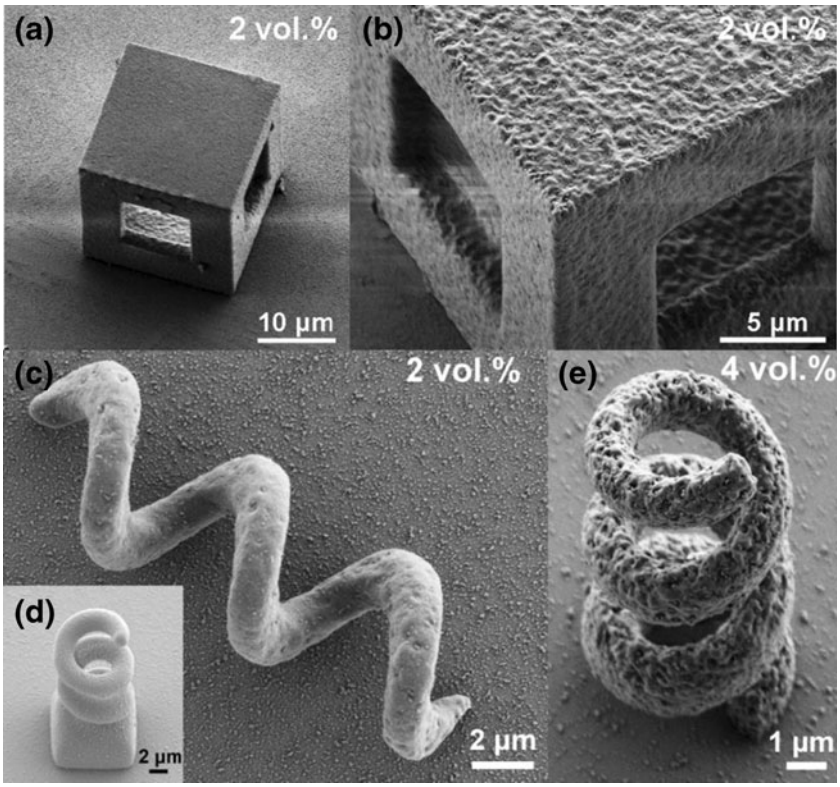

Fig. 4 SEM images from MPC hollow cube (20×20×20 μm with 2 μm wall thickness and four 10×10 μm windows) with 2 vol.% Fe_3O_4 nanoparticle concentration (**a**). Closer view of the cube (**b**). Helical microstructure with 2 vol.% Fe_3O_4 nanoparticle concentrations (**c**) and with a cube-like base for better fixation to the substrate (**d**). **e** Helical microstructure with 4 vol.%

superparamagnetic MPC microstructures with 2 vol.% filler concentration rotate along the axial direction of the microstructure. The swim performance near the substrate surface is characterized by two motions, i.e. forward and drift translation. The image sequence in Fig. 5a shows a complete rotation of the structure around its helical axis. Figure 5b shows a swim displacement of approximately 12 μm (forward plus drift motion) during 4 s. The cube on the bottom of the helical structure was used as an anchor during fabrication as seen in Fig. 4d, while helical microstructures without cubes were also fabricated and showed similar swimming behavior. This experiment shows that an actuation and magnetic control of microstructures made from the superparamagnetic MPC with only 2 vol.% nanoparticles concentration is possible. To achieve a rotation of the helical microstructure a magnetic torque along the helical axis must act on the structure. The torque applied on the helical microstructure is given by

$$T_m = V\mathbf{M} \times \mathbf{B} \tag{1}$$

where V and $\boldsymbol{M}$ are the volume (m^3) and magnetization (A/m) of the body, respectively, and $\boldsymbol{B}$ is the applied magnetic flux density (T). To produce a torque about the axis of the helical structure there must be a component of magnetization in the

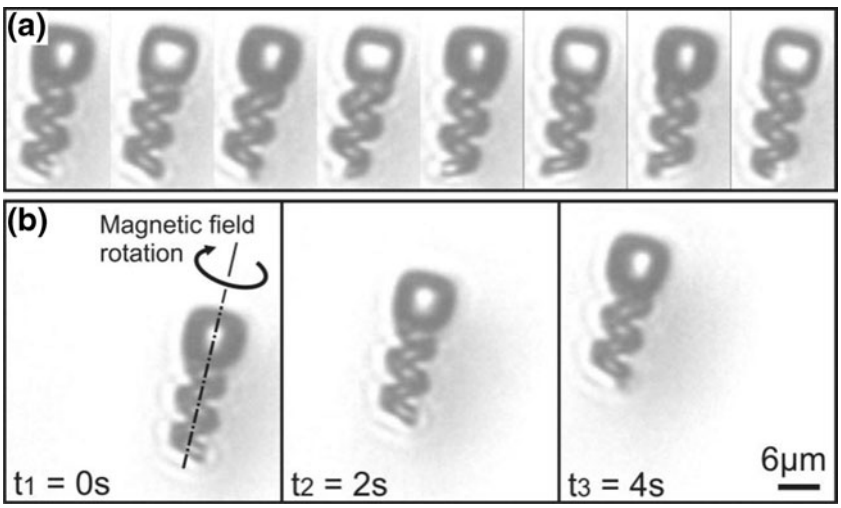

Fig. 5 Swim test in water of MPC helical structures with 2 vol.% Fe_3O_4 superparamagnetic nanoparticle concentration. **a** Microscope image sequence showing a full rotation of the helical structure around its helical axis. **b** Microscope image sequence showing propulsion of the helical structure. The magnetic field strength and input frequency were set to 8mT and 4Hz, respectively. A distance of approximately 12 μm (forward plus drift motion) was covered in 4 s

radial direction. The magnetization depends on the magnetic anisotropy (i.e., shape anisotropy) of the helical microstructure. Different possibilities for controlling the magnetic anisotropy of the helical microrobots have been reported previously, such as using permanent magnetic materials (Ghosh and Fischer 2009) or adding a magnetic head plate 15. This work shows that it is possible to generate an actuation torque for a helical microstructure even without controlling the magnetic anisotropy.

3 Conclusions

Superparamagnetic microstructures with various shapes, such as hollow cubes and helical structures, were fabricated using TPP technology with a superparamagnetic polymer composite with up to 4 vol.% (15 wt.%) concentration of Fe_3O_4 nanoparticles. In comparison to conventional UV-based photolithography, the aspect ratio and resolution of the MPC microstructures were significantly improved using TPP. It was demonstrated that MPC microstructures are non-toxic to cells and have potential for *in vitro* biomanipulation. Furthermore, the MPC helical microstructures, embedded with randomly distributed magnetic nanoparticles, are capable of performing corkscrew motion using a rotating field, and swimming can be controlled precisely in three dimensions. An advantage compared to permanently magnetized swimmers is that due to superparamagnetic characteristics the swimmers do not magnetically attract each other, when the external magnetic field is turned off. The three dimensional MPC microstructures could act as microrobots for biomedical applications, such as single-cell manipulation and robotic drug delivery platforms, which have high operation flexibility in the fluidic environment, such as pH and temperature, and with versatile functionalization by surface modification techniques (Deepu et al. 2009).

4 Experimental section

4.1 Preparation of magnetic polymer composite

The magnetic polymer composite (MPC) is made from epoxy SU-8 polymer containing magnetite nanoparticles with diameters of 11.4±3.4 nm (average diameter measured by TEM). The preparation detail of MPC was published elsewhere (Suter et al. 2011b).

4.2 Cytotoxicity tests of MPC

Cell culture The cytotoxicity tests were conducted using normal human dermal fibroblasts (NHDF, PromoCell, Germany). The proliferation of such cells was harvested from exponentially growing subconfluent monolayers. The culture was maintained in 25 cm^2 culture flasks in DMEM (Cat. No. 21885, low glucose, glutamax I, GibcoBRL) supplemented

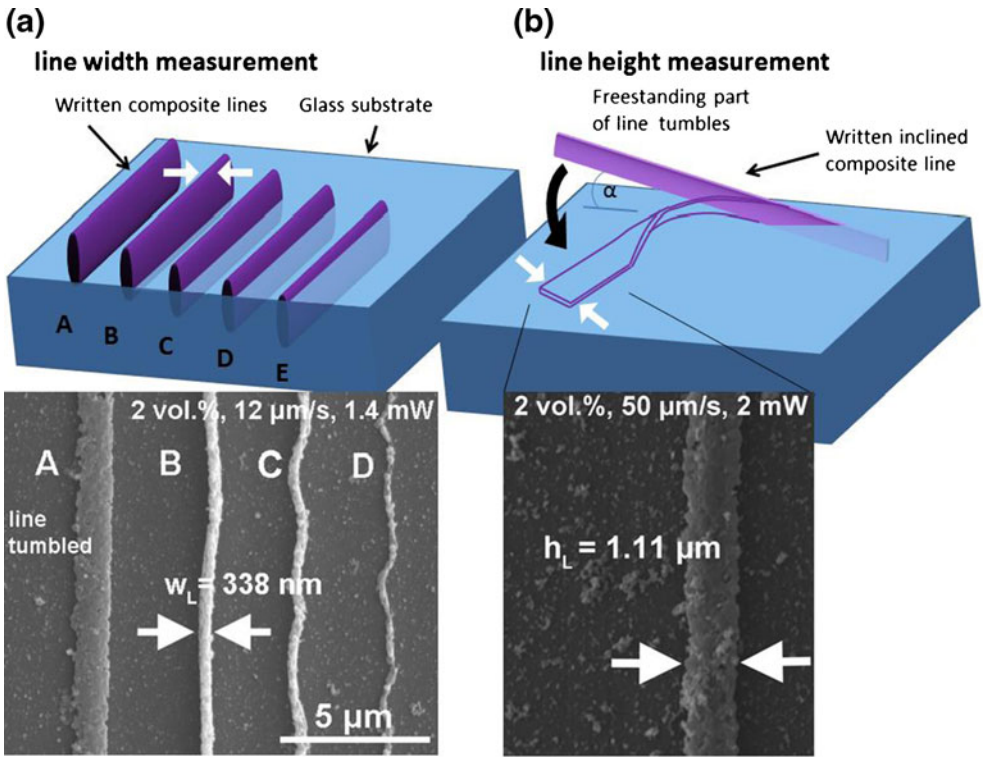

Fig. 6 **a** 2 vol.% MPC lines with different offsets to the glass substrate are written to determine the linewidth, w_L, using SEM. **b** Inclined MPC lines are written with an angle $\alpha \approx 5°$ to the substrate. After development and air drying process the polymerized line tumbles onto the substrate. The height of the line, h_L, can be measured by SEM

with 10 % heat inactivated FBS (F7524, Sigma) and 1 % ABAM (Cat. No. 15240, GibcoBRL) at 37 °C and 5 % CO_2. Cells were used until passage 20.

Live and dead staining Three thousand NHDFs were cultured on individual surfaces for a total time of 24 h in a 24-well-plate and stained with FDA (fluorescein diacetate, 1 mg/ml, 1:1000, Fluka) and Hoechst 33342 nuclear stain in PBS (Invitrogen, 1:1000) for 10 min at room temperature. Living cells metabolize FDA to fluorescein, which can be detected with a FITC-filter of an epi-fluorescence microscope. With Hoechst 33342 nuclear stain the total number of cells is detected by a DAPI filter. The samples were washed 3 times with PBS and analyzed by fluorescence microscopy (Zeiss Axiovert 200 M) (Suter et al. 2012).

Cytotoxicity The cytotoxicity of different surfaces of MPC with a nanoparticle concentration of 0, 1, 2, 3, 5, and 10 vol.% was determined by the mitochondrial activity of living cells using WST-1-proliferation assay (Roche). Surfaces were sterilized for at least 20 min under UV-light and stored for 2 h in PBS (phosphate buffered saline, 0.1 M, pH 7.4). 3000 NHDFs were cultured on individual surfaces for a total time of 24 h in 24-well plates (TPP, Switzerland) in a total volume of 500 ml medium. 24 h after seeding mitochondrial activity was measured by the addition of 50 ml WST-1 solution per 24-well and WST-1 absorption was analyzed at 440 nm using a microplate reader Infinite M200 (Tecan). As controls 3000 NDHFs were cultured on tissue culture polystyrene (TCPS) in a similar way. Each condition was performed in duplicates and repeated 2 times.

4.3 Fabrication of 3D microdevices using TPP

The MPC microstructures were fabricated by a direct laser writing tool from the company Nanoscribe GmbH with a Ti:sapphire near IR femtosecond laser (100 MHz repetition rate, sub-150 fs pulses, central wavelength of 780 nm). To achieve MPC microstructures with smallest feature sizes an oil immersion objective with 100× magnification (NA=1.4) was used.

The MPC suspension was deposited by spin-coating (layer of 10–30 μm) on a 170 μm thick glass substrate. The prebaking for spin-coated samples was done at 95 °C for 15 min. Prebaking was used to obtain a lower solvent concentration in the MPC. After exposure by TPP all the samples were postbaked at 95 °C for 3 min to perform the polymerization. Then, the composite was developed in resist developer mr-DEV 600 for 5 to 10 min, rinsed with isopropanol and dried at air. Samples with Fe_3O_4 particle concentration of 0, 2, 4 vol.% were prepared.

4.4 Measuring of minimal line width and height

The minimal line width is determined by measuring the width of a written MPC line after development. The lines have an elliptical cross-section, and the thickness is measured at the widest position. As the laser focus cannot be precisely adjusted relative to the substrate surface, lines with different offsets in z-direction were written (Fig. 6a). The line width, w_L, is measured by scanning electron microscopy (SEM) at the highest or second highest undetached line. For determining the minimal line height, h_L, inclined lines were written with different scanning speed and laser power from the substrate as illustrated in Fig. 6b. During air drying after developing the freestanding lines tumble onto the side towards the substrate, and the line height can be measured by SEM.

4.5 Magnetic actuation using 3-axis Helmholtz electromagnetic coils setup

A uniform rotating magnetic field was used to test the actuation and swimming properties of the MPC-based microstructures. The setup consists of three Helmholtz coil pairs placed orthogonally to each other producing uniform field in any direction (Zhang et al. 2009b; Zhang et al. 2010b). The field can be rotated by varying the currents through the coils. The MPC microstructure was immersed in a water tank. The structure can be observed by an optical microscope. To investigate the swimming properties, the microstructure was mechanically detached from the glass substrate. The motion was recorded using a CCD camera placed on top of the microscope.

Acknowledgments The authors thank Eszter Barthazy and Elisabeth Müller (EMEZ at ETH Zurich) for the TEM-images, the technical support from the FIRST lab at ETH Zurich. Funding for this research is provided by Swiss National Science Foundation (SNSF), project number 130069 and the ETH Zurich (TH-28 06–3).

References

R.A. Anderson, H.C. Berg, Bacteria swim by rotating their flagellar filaments. Nature **245**, 380–382 (1973)

M. Colombo, S. Carregal-Romero, M.F. Casula, L. Gutierrez, M.P. Morales, I.B. Bohm, J.T. Heverhagen, D. Prosperi, W.J. Parak, Biological applications of magnetic nanoparticles. Chem. Soc. Rev. **41**, 4306–4334 (2012)

A. Deepu, V.V.R. Sai, S. Mukherji, Simple surface modification techniques for immobilization of biomolecules on SU-8. J. Mater. Sci. **20**, 25–28 (2009)

D.L. Fan, Z.Z. Yin, R. Cheong, F.Q. Zhu, R.C. Cammarata, C.L. Chien, A. Levchenko, Subcellular-resolution delivery of a cytokine through precisely manipulated nanowires. Nat. Nanotechnol. **5**, 545–551 (2010)

E. Frances, J. Burdan, A. Cutino, K.E. Green, A new sustained delivery technology for posterior eye disease. Expert Opin. Drug Deliv. **5**, 1039–1046 (2008)

A. Ghosh, P. Fischer, Controlled propulsion of artificial magnetic nanostructured propellers. Nano Lett. **9**, 2243–2245 (2009)

M. Hagiwara, T. Kawahara, Y. Yamanishi, T. Masuda, L. Feng, F. Arai, On-chip magnetically actuated robot with ultrasonic vibration for single cell manipulations. Lab Chip **11**, 2049–2054 (2011)

J. Kim, H.S. Kim, N. Lee, T. Kim, H. Kim, T. Yu, I.C. Song, W.K. Moon, T. Hyeon, Multifunctional uniform nanoparticles composed of a magnetite nanocrystal core and a mesoporous silica shell for magnetic resonance and fluorescence imaging and for drug delivery. Angew. Chem. Int. Ed. **47**, 8438–8441 (2008)

A.H. Lu, E.L. Salabas, F. Schuth, Magnetic nanoparticles: synthesis, protection, functionalization, and application. Angew. Chem. Int. Ed. **46**, 1222–1244 (2007)

S. Martel, M. Mohammadi, O. Felfoul, Z. Lu, P. Pouponneau, Flagellated magnetotactic bacteria as controlled MRI-trackable propulsion and steering systems for medical nanorobots operating in the human microvasculature. Int. J. Robot. Res. **28**, 571–582 (2009)

Y.F. Mei, A.A. Solovev, S. Sanchez, O.G. Schmidt, Rolled-up nanotech on polymers: from basic perception to self-propelled catalytic microengines. Chem. Soc. Rev. **40**, 2109–2119 (2011)

B.J. Nelson, I.K. Kaliakatsos, J.J. Abbott, Microrobots for minimally invasive medicine. Annu. Rev. Biomed. Eng. **12**, 55–85 (2010)

G.A. Ozin, I. Manners, S. Fournier-Bidoz, A. Arsenault, Dream Nanomachines. Adv. Mater. **17**, 3011–3018 (2005)

S.H. Park, D.Y. Yang, K.S. Lee, Two-photon stereolithography for realizing ultraprecise three-dimensional nano/microdevices. Laser Photonics Rev. **3**, 1–11 (2009)

C. Peters, O. Ergeneman, B. J. Nelson, C. Hierold, Pushing the limits of photo-curable SU-8-based superparamagnetic polymer composites, *Proc. Int. Conf. on Solid-State Sensors, Actuators and Microsystems Conference (TRANSDUCERS)* (Barcelona, 2013), pp 2676–2679

K.E. Peyer, L. Zhang, B.J. Nelson, Bio-inspired magnetic swimming microrobots for biomedical applications. Nanoscale **5**, 1259–1272 (2013a)

K.E. Peyer, S. Tottori, F. Qiu, L. Zhang, B.J. Nelson, Magnetic helical micromachines. Chem. Eur. J. **19**, 28–38 (2013b)

E.M. Purcell, Life at low Reynolds number. Am. J. Phys. **45**, 3–11 (1977)

F.M. Qiu, L. Zhang, S. Tottori, K. Marquardt, K. Krawczyk, A. Franco-Obregon, B.J. Nelson, Bio-inspired microrobots: the first intimate contact with cells. Mater. Today **15**, 463 (2012)

S. Schuerle, S. Pane, E. Pellicer, J. Sort, M.D. Baro, B.J. Nelson, Helical and tubular lipid microstructures that are electroless-coated with CoNiReP for wireless magnetic manipulation. Small **8**, 1498–1502 (2012)

J.J. Shi, D. Ahmed, X. Mao, S.C.S. Lin, A. Lawit, T.J. Huang, Acoustic tweezers: patterning cells and microparticles using standing surface acoustic waves (SSAW). Lab Chip **9**, 2890–2895 (2009)

C.E. Sing, L. Schmid, M.F. Schneider, T. Franke, A. Alexander-Katz, Controlled surface-induced flows from the motion of self-assembled colloidal walkers. Proc. Natl. Acad. Sci. U. S. A. **107**, 535–540 (2010)

K.M. Sivaraman, C. Kellenberger, S. Pane, O. Ergeneman, T. Luhmann, N.A. Luechinger, H. Hall, W.J. Stark, B.J. Nelson, Porous polysulfone coatings for enhanced drug delivery. Biomed. Microdevices **14**, 603–612 (2012)

A.A. Solovev, W. Xi, D.H. Gracias, S.M. Harazim, C. Deneke, S. Sanchez, O.G. Schmidt, Self-propelled nanotools. ACS Nano **6**, 1751–1756 (2012)

M. Suter, O. Ergeneman, J. Zurcher, C. Moitzi, S. Pane, T. Rudin, S.E. Pratsinis, B.J. Nelson, C. Hierold, A photopatternable superparamagnetic nanocomposite: material characterization and fabrication of microstructures. Sensors Actuat. B Chem. **156**, 433–443 (2011a)

M. Suter, O. Ergeneman, J. Zurcher, S. Schmid, A. Camenzind, B.J. Nelson, C. Hierold, Superparamagnetic photocurable nanocomposite for the fabrication of microcantilevers. J. Micromech. Microeng. **21**, 025023 (2011b)

M. Suter, Photopatternable superparamagnetic nanocomposite for the fabrication of microstructures, Ph.D. dissertation, ETH Zurich, (2012)

Y. Tian, Y.L. Zhang, J.F. Ku, Y. He, B.B. Xu, Q.D. Chen, H. Xia, H.B. Sun, High performance magnetically controllable microturbines. Lab Chip **10**, 2902–2905 (2010)

S. Tottori, L. Zhang, F.M. Qiu, K.K. Krawczyk, A. Franco-Obregon, B.J. Nelson, Magnetic helical micromachines: fabrication, controlled swimming, and cargo transport. Adv. Mater. **24**, 811–816 (2012)

J. Wang, Cargo-towing synthetic nanomachines: towards active transport in microchip devices. Lab Chip **12**, 1944–1950 (2012)

H. Xia, J.A. Wang, Y. Tian, Q.D. Chen, X.B. Du, Y.L. Zhang, Y. He, H.B. Sun, Ferrofluids for fabrication of remotely controllable micro-nanomachines by two-photon polymerization. Adv. Mater. **22**, 3204–3207 (2010)

L. Zhang, J.J. Abbott, L.X. Dong, B.E. Kratochvil, D. Bell, B.J. Nelson, Artificial bacterial flagella: fabrication and magnetic control. Appl. Phys. Lett. **94**, 064107 (2009a)

L. Zhang, J.J. Abbott, L. Dong, K.E. Peyer, B.E. Kratochvil, H. Zhang, C. Bergeles, B.J. Nelson, Characterizing the swimming properties of artificial bacterial flagella. Nano Lett. **9**, 3663–3667 (2009b)

Y.L. Zhang, Q.D. Chen, H. Xia, H.B. Sun, Designable 3D nanofabrication by femtosecond laser direct writing. Nano Today **5**, 435–448 (2010a)

L. Zhang, K.E. Peyer, B.J. Nelson, Artificial bacterial flagella for micromanipulation. Lab Chip **10**, 2203–2215 (2010b)